HYDRODINAMIC BEHAVIOR
IN A LABORATORY SCALE INTERNAL AIRLIFT OPERATING UNDER HOMOGENEOUS REGIME

Patrícia A. S. Monteiro
University of São Paulo, Physical Institute of São Carlos, São Paulo, Brazil
pamarasantiago@gmail.com

Glauber Cruz
University of São Paulo, Engineering School of São Carlos, Mechanical Engineering Department, São Paulo, Brazil
glauber.cruz@usp.br

Paulo Seleghim Jr.
University of São Paulo, Engineering School of São Carlos, Mechanical Engineering Department, São Paulo, Brazil
seleghim@sc.usp.br

Abstract. Pneumatic bioreactors have shown great potential for biotechnological processes, because not utilize moving parts in its construction and operation, and there is a lower power consumption when compared to conventional stirred tank bioreactors. These bioreactors are widely used in processes that require continuous contact between two phases, gas and liquid, due to their excellent heat and mass transfer characteristics. However, the process of designing, building and evaluating bioreactors for high-substrate concentration process, as enzymatic hydrolysis process of sugarcane bagasse, is both costly and time consuming. The use of a computational fluid dynamics (CFD) model can aid in bioreactor development by providing detailed information on the hydrodynamic and chemical environments necessary for optimal process. The aim of this work was to compare performance in an internal loop airlift reactor and identify the flow pattern. For this study, the ANSYS CFX 13.0 commercial computational fluid dynamics package was used to predict the flow pattern. Parameters evaluated were averaged liquid circulation velocity and overall gas holdup. In these simulations the conditions adopted were: dispersed phase (gas) - air; phase continuous (liquid) -water; drag model: Grace and different air superficial velocities (Ug). A two-phase flow model provided by the bubbly flow application mode was employed in this project. In the liquid phase, the turbulence can be described using the k-ε model. Through this study, it was possible to obtain useful and ssential information about the design and operation of this equipment.

Key words: airlift, computational fluid dynamic (CFD), liquid circulation velocity, overall gas holdup, air sparger.

1. INTRODUCTION

Airlift reactors is the main types pneumatically agitated reactors. They possess good mixing, mass and heat transfer characteristics and they are used in a wide range of industrial applications such as waste water treatment, chemical (e.g. hydrogenations and oxidations) and biochemical processes, and others. The other advantages are simplicity of construction, absence of moving parts, and low power consumption. Their other advantageous features in case of biochemical processes are ease of long term sterile operation, and a hydrodynamic environment suitable for fragile biocatalysts, which are susceptible to physical damage by fluid turbulence or mechanical agitation (Chisti, 1998).

Airlift reactors are one of the most important types of modified bubble columns (BCs) and there are two types of ALR: internal and external loop. Internal loop reactors consist of concentric tubes or split vessels, in which a part of the gas is entrained into the downcomer, whereas external loop reactors are two conduits connected at the top and the bottom, in which little or no gas recirculates into the downcomer. The part in which the sparger is located is called the riser, and the other is the downcomer. The driving force, based on the static pressure difference, or the mixture density difference, between the riser and the downcomer generates the loop liquid circulation. Compared with conventional reactors, such as stirred tank reactors or bubble columns, shear stress is relatively constant and mild throughout the reactor (van Baten *et al.*, 2003). In the design of airlift reactors, the geometry of the system plays an important role in its efficiency for mixing and mass transfer. Thus, two key hydrodynamic parameters of airlift reactors are the gas holdup and liquid circulation velocity. The knowledge of the airlift hydrodynamics is needed for the design of the airlift reactor (Ebrahimifakhar *et al.*, 2011). The hydrodynamic and other relevant parameters such as the airlift geometry are interrelated and their relationship can be quite complex and they directly or indirectly influence each other in sometimes not so obvious ways (Chisti, 1998), e.g. the driving force for the liquid circulation is the difference in gas holdups between the riser and the downcomer. This driving force is balanced by friction losses in the riser and the downcomer and in the bottom and top parts of the reactor (influence of bottom and top clearances in the case of internal loop airlifts or losses in connecting pipes in the case of external airlifts and of the airlift geometry in general). However, the

resulting liquid circulation in turn affects the riser and downcomer gas holdup and thus the driving force. The gas holdup depends also on bubble slip velocity, which depends on the bubble size. Bubble size is influenced by the gas distributor, coalesce properties of the involved fluids and by turbulence. Turbulence is influenced by liquid circulation, etc (Simcik *et al.*, 2011).

Computational fluid dynamics (CFD) is one of the most powerful tools for analyzing and optimizing results and can save a great deal of time and expense (Ebrahimifakhar *et al.*, 2011). Several recent publications have established the potential of computational fluid dynamics (CFD) for describing the hydrodynamics of bubble columns and airlifts (Simcik *et al.*, 2011; Ebrahimifakhar *et al.*, 2011; van Baten *et al.,* 2003; van Baten and Krishna, 2001; Wasewar *et al.*, 2008; Zhang *et al.*, 2012).

The objective of the present work was to study, using of the CFD (computational fluid dynamics) simulation, the hydrodynamics (liquid circulation velocity and on the gas holdup) in an internal loop airlift reactor with air injection between the cylinders (annulus). The introduction of air was performed for 18 holes located near the outer cylinder wall. In the simulations were employed different gas superficial velocities.

2. MATERIAL AND METHODS

2.1 Reactors configuration and operating conditions

The simulations were done in an internal loop airlift reactor with air injection between the cylinders (annulus) (Figure 1). The total volume of the apparatus was 5 L. The outer cylinder has a diameter of 0.115 m and a height of 0.6 m, and the inner cylinder, or the draft tube (downcomer), has a diameter of 0.08 m, a height of 0.35 m and this is mounted into the column 0.03 m above at the bottom. At the bottom of the column, the gas phase is introduced through a circular holes arranged near the outer cylinder with 18 holes of 0.38mm diameter. This equipment has a sparger to the gas inlet, the more efficient than conventional ones, for example, ring-type nozzles, perforated plates and spider type.
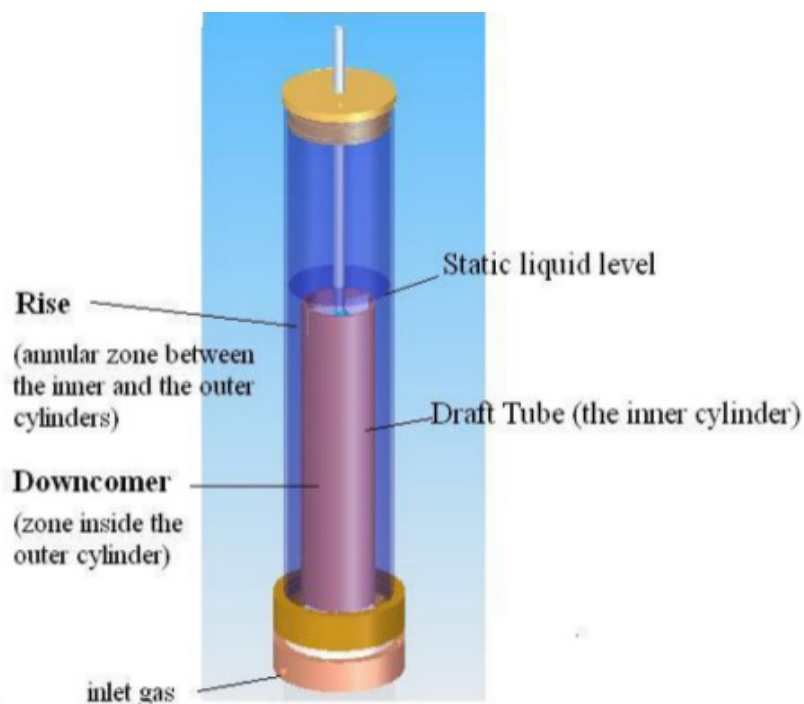
Figure 1. Schematic representation of the internal loop airlift reactor.

2.2 Mathematical modeling

In the present work, an Euler–Euler two-fluid model was employed to investigate the hydrodynamics of gas–liquid phases in the internal loop airlift reactor because of the obvious computational advantages of this model at high dispersed phase volume fractions. In this model, liquid is considered to be the continuous phase, and gas bubbles are considered to be the dispersed phase. Two fluids are considered to be incompressible, and the uniform pressure field is

assumed to be shared by both phases. Simulations were performed for transient state, the simulation time of 120 s and time step of 0.001s. The physical properties of the gas and liquid phases (at 25 ^{o}C) are specified in Tab. 1.

Table 1. Properties used in the CFD simulations.

	Liquid (water)	Gas (air)
Viscosity [cP]	8.9×10^{-1}	1.831×10^{-2}
Density (ρ) [kg m^{-3}]	997	1.185
Surface tension (σ) [N m^{-1}]	0.072	

The conditions adopted were dispersed phase (gas) air; continuous phase (liquid) water. The drag model used was from Grace (Santos, 2005) and liquid phase turbulence was modeled using the k-ε model. The governing equations of mass and momentum balance are solved for each phase and can be written as follows.

2.2.1 Continuity equations

$$\frac{\partial(\alpha_i\rho_i)}{\partial t} + \nabla \cdot (\alpha_i\rho_i\overline{u_i}) = S_i \qquad (i=g, l) \tag{1}$$

where i denotes the gas or liquid phase; t is the time, and ρ_i, u_i and α_i are the density, velocity vector and volume fraction of phase i, respectively. The mass source term Si on the right side of Eq. (1) is zero because interphase mass transfer is not taken into consideration in this model. The total sum of phasic volume fractions should satisfy the condition of unity (Zhang *et al.*, 2012).

2.2.2 Momentum equations

$$\frac{\partial(\alpha_i\rho_i\overline{u_i})}{\partial t} + \nabla \cdot (\alpha_i\rho_i\overline{u_i}\,\overline{u_i}) = -\alpha_i\nabla\rho + \nabla \cdot \left(\alpha_i\mu_{eff,i}\left(\nabla\overline{u_i} + (\nabla\overline{u_i})^T\right)\right) + \alpha_i\rho_i\vec{g} + M_{I,i} \tag{2}$$

where ρ is the pressure field, μ_{eff} is the effective viscosity, g is the gravitational acceleration vector, and M_I is the interphase momentum exchange force (Zhang *et al.*, 2012).

2.2.3 Closure law for interphase momentum exchange

For the momentum transfer, the said closure is provided by the momentum transfer, which is given by the drag force between the phases. For gas–liquid flows, important interfacial forces include drag, lift, virtual mass, rotation and strain forces.

In the system of bubble columns, the amount of movement in the system is provided by the rising of the dispersed phase (d, gaseous) to the rise, due to the buoyant force provides energy (momentum) to the continuous phase (c, liquid). The drag force is the force that acts on the dispersed phase and the continuous phase is given by Eq. (3) (Santos, 2005).

$$F_D = \frac{3}{4}\alpha_g\rho_i\frac{C_D}{d_b}\left|\overline{u_g} - \overline{u_l}\right|\left(\overline{u_g} - \overline{u_l}\right) \tag{3}$$

where C_D is the drag force coefficient between liquid and gas phases, and db is the equivalent diameter of the bubbles. Bubble diameter is set as uniform at 7 mm.

Many different correlations can be found in the literature to compute the drag force coefficient. The most widely used drag force correlation proposed by Grace was used in this work. As in Ishii-Zuber model, the model de Grace consider the effect of the shape of the dispersed phase in the calculation of the coefficient of drag. This model assumes that the bubble has constant interfacial tension.

For Grace model equation for the C_D (ellipse) is given by Eq. (4) (Santos, 2005).

$$C_D = \frac{4}{3}\frac{gd_b\Delta\rho}{\overline{U_t}^2\rho_l} \tag{4}$$

where U_t is the terminal velocity of rise of a bubble and is given by Eq. (5).

Patrícia A. S. Monteiro, Glauber Cruz and Paulo Seleghim Jr
Hydrodynamic behavior in a laboratory scale airlift operating under homogeneous regime

$$\overrightarrow{U_t} = \frac{\mu_l}{\rho_l d_b} M^{-0.149} (J - 0.857) \tag{5}$$

where, M is Morton number (dimensionless) (Eq. 6)

$$M = \frac{\mu_l^4 g \Delta p}{\rho^2 \sigma^3} \tag{6}$$

where σ is surface tension [N m^{-1}]; and

$$J = \begin{cases} 94H^{0.751} & 2 < H \le 59.3 \\ 3.42H^{0.441} & H > 59.3 \end{cases} \tag{7}$$

where, $H = \frac{4}{3} E_o M^{-0.149} \left(\frac{\mu_l}{\mu_{ref}} \right)^{-0.14}$, E_0 is Eotvos number (dimensionless), $E_0 = \frac{g \rho_l d_b^2}{\sigma}$, μ_{ref} = 0.0009 Kg m^{-1}s^{-1} (water value).

2.2.4 Closure law for turbulence

In this study, the superficial gas velocities are relatively low, the concentration of the dispersed gas phase is dilute, and the liquid is clearly the primary continuous phase, so the dispersed standard k–ε model was used to model turbulence. The effective viscosity of the liquid phase in Eq. (2) consists of the molecular viscosity and the turbulence viscosity ($\mu_{t,l}$) of the liquid phase and is described by Eq. (8).

$$\mu_{eff,l} = \mu_l + \mu_{t,l} \tag{8}$$

The turbulence viscosity of the liquid phase is calculated by Eq. (9).

$$\mu_{t,l} = C_\mu \rho_l \left(\frac{k_l^2}{\varepsilon_l} \right) \tag{9}$$

where C_μ = 0.09, k_l and ε_l are turbulence kinetic energy and the turbulence dissipation rate, respectively, and are obtained by solving the scalar transport equations (Eq. 10 and 11).

$$\frac{\partial (\alpha_l \rho_l k_l)}{\partial t} + \nabla \cdot (\alpha_l \rho_l \overline{u_l} k_l) = \nabla \cdot \left(\alpha_l \frac{\mu_{t,i}}{\sigma_k} \nabla k_l \right) + \alpha_l G_{k,i} - \alpha_l \rho_l \varepsilon_l + \alpha_l \rho_l \prod_{kl} \tag{10}$$

$$\frac{\partial (\alpha_l \rho_l \varepsilon_l)}{\partial t} + \nabla \cdot (\alpha_l \rho_l \overline{u_l} \varepsilon_l) = \nabla \cdot \left(\alpha_l \frac{\mu_{t,i}}{\sigma_\varepsilon} \nabla \varepsilon_l \right) + \alpha_l \frac{\varepsilon_l}{k_l} (C_{1\varepsilon} G_{k,l} - C_{2\varepsilon} \rho_l \varepsilon_l) + \alpha_l \rho_l \prod_{gl} \tag{11}$$

The standard constants used in the turbulence equations are $C_{1\varepsilon}$ = 1.44, $C_{2\varepsilon}$ = 1.92, σ_k = 1.0 and σ_ε = 1.3. $G_{k,l}$ is the production of turbulent kinetic energy, $\prod_{kl}$ and $\prod_{\varepsilon l}$ represent the influence of the dispersed phase on the continuous phase. All the definitions for these terms can be found in CFX guide (CFX, 2011) (Zhang *et al*., 2012; van Baten *et al*., 2003; Wasewar *et al*., 2008).

2.3 Boundary conditions

In this work, the entire internal airlift reactor was employed as the computational domain. At the inlet, the boundary conditions were specified by the superficial gas velocity. Superficial gas velocities (U_g) were varied from 0.004 - 0.22 m s^{-1} for the simulation. The outlet was considered to be at atmospheric pressure so the gas coming out of the reactor can exit freely. The boundary conditions were a no-slip condition for liquid and a free-slip condition for the gas phase on all reactor walls. Isothermal conditions are assumed in the computational domain, so the energy equation is not calculated. Mass transfer and chemical reactions were neglected. In this work, simulations were performed using the program commercial computational fluid dynamics (CFX 13.0 - ANSYS).

3. DEFINITIONS

3.1 Superficial gas velocity (V_G):

It is a velocity at which gas passes upwards through (liquid filled) stirred tank. It is calculated as follows.

$$\text{superficial gas velocity}\left(ms^{-1}\right)=\frac{\text{volumetric flow rate of gas}\left(m^3 s^{-1}\right)}{\text{cross sectional area riser}\left(m^2\right)} \quad (12)$$

3.2 Gas hold up (ε_g)

It is the ratio of gas phase volume to total volume. Gas holdup is an important hydrodynamic parameter and is a basic measure of gas-liquid contacting airlift reactor. Gas hold up is governed by average bubble size, population of bubbles and bubble velocity. The interfacial area and mass transfer rate are dependent on holdup. Holdup also indicates the volume fraction of gas phase and mean residence time of the gas phase in the vessel. It also governs the velocity or flow field in the vessel, turbulence characteristics in the individual phases and the energy dissipation rates. Thus a study of gas holdup is important for scaling up and design of airlift reactors.

4. RESULTS AND DISCUSSIONS

The hydrodynamics simulation results at different superficial gas velocities for the internal loop airlift reactor are presented here.

Figure 2 show the volume fraction of air at superficial velocities in riser (U_{GS}) in the reactor. The gas was injected homogeneously over the bottom region. The air bubbles move upwards due to the differences of density between the gas and liquid phases. The simulation time, represented in the figure, is 120 s.
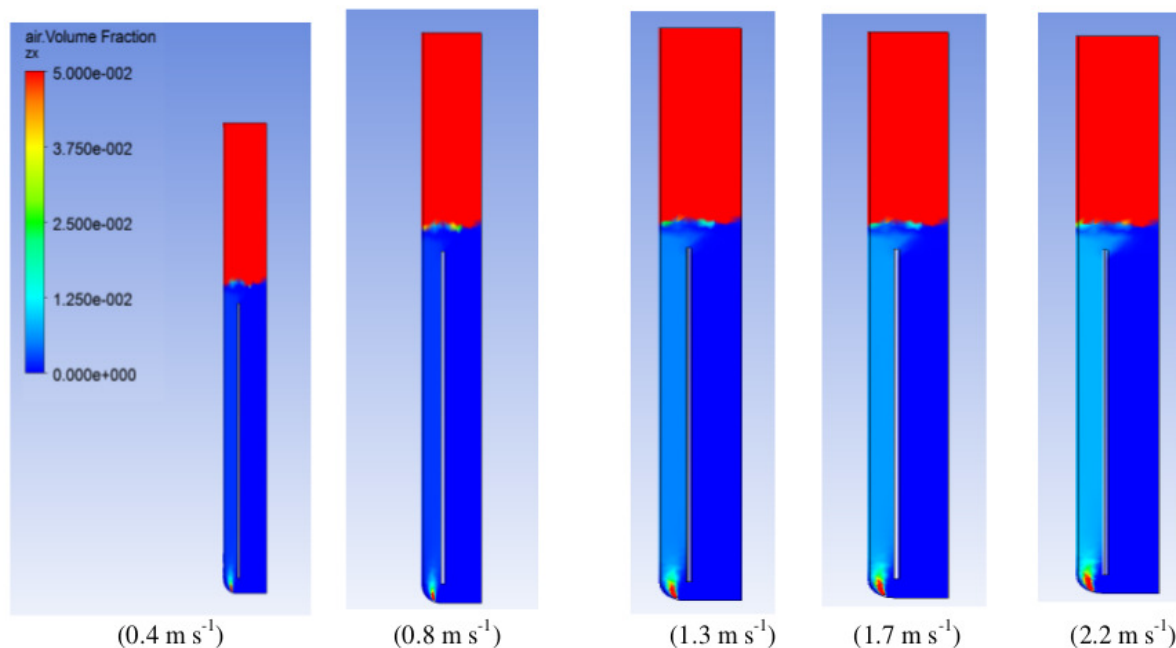
Figure 2. Volume fraction of gas at various superficial velocities in riser.

Through Figure 2 shows that for low UGS values that all the volume fraction of gas present the reactor is in the riser region defining the arrangement type I. In this type of regime, the gas is not present in the downcomer region. This regime occurs only at low volumetric flow rates of gas feed (Q_G), when the liquid velocity is not sufficient to drag bubbles to the downcomer region (van Benthum *et al.*, 1999).

Through Figure 3 was possible to verify that increasing the total gas holdup in the reactor increases with the increasing superficial gas velocities in the range of this study (0.004 - 0.22 m s^{-1}).

Patrícia A. S. Monteiro, Glauber Cruz and Paulo Seleghim Jr
Hydrodynamic behavior in a laboratory scale airlift operating under homogeneous regime
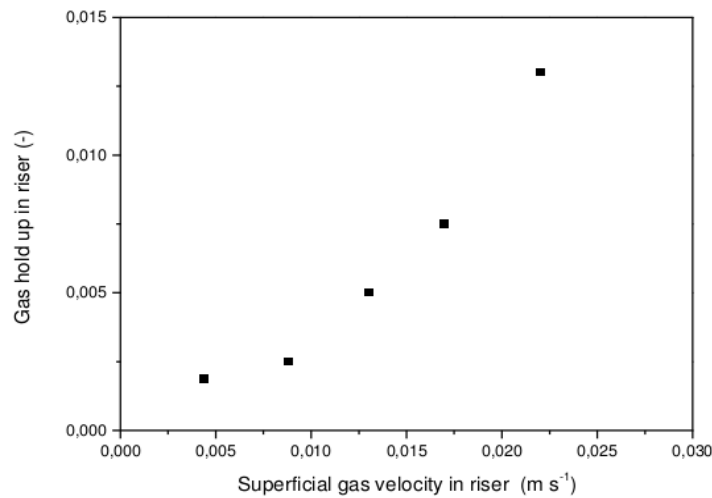
Figure 3. Simulations results data for the gas hold up in riser

Figure 4 show the liquid velocity (U_L) at superficial velocities in riser (U_{GS}) in the reactor.
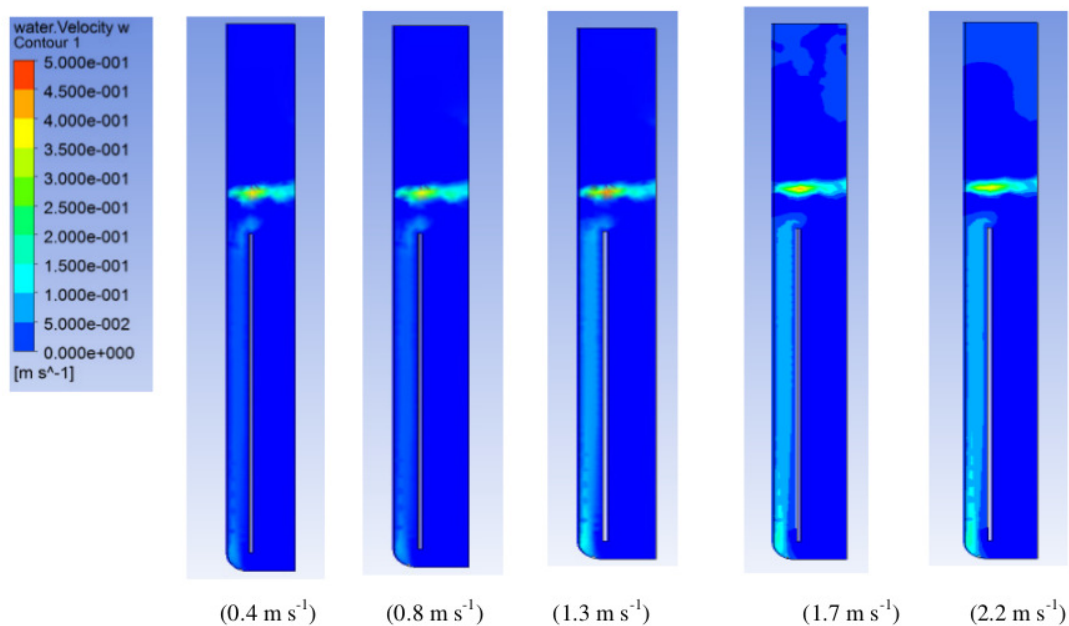
Figure 4. Comparison of the liquid velocity (m s^{-1}) at various superficial velocities in riser.

From the results obtained (Figures 4 and 5) it was verified that at low superficial gas velocities ($U_{GS} < 0.02$ m s^{-1}), the velocity (U_L) increased significantly with increase of U_{GS} and U_{GS} values greater than 0.02 m s^{-1}, the increase U_L with U_{GS} was less intense. This is due to the fact that the gas does not achieves more momentum transfer to the liquid, as well as difference between the gas retention in regions of riser and downcomer decrease with increasing U_{GS}. Thus, there is no more a difference significant densities between these two regions, which is the driving force for circulating the liquid.

Similar results were reported by Zhang *et al*., (2012) and Chisti e Haza, (2002). Zhang *et al*., (2012) observed that when superficial gas velocities are less than 1 cm/s, the liquid velocity increases rapidly with the increasing superficial gas velocity. However, when the superficial gas velocity is beyond 1 cm/s, the increasing rate of liquid velocity becomes slow, probably because, at low superficial gas velocity ranges, the gas holdup in the riser increases rapidly while the gas holdup in the downcomer does not increase in an obvious manner because bubbles can hardly be entrained into the downcomer. The increased difference in gas holdup between the riser and the downcomer leads to the increasing liquid velocity in the downcomer. As the superficial gas velocity is over 1 cm. s^{-1}, bubbles begin to be increasingly entrained into the downcomer. This phenomenon can also be observed in the experiment.
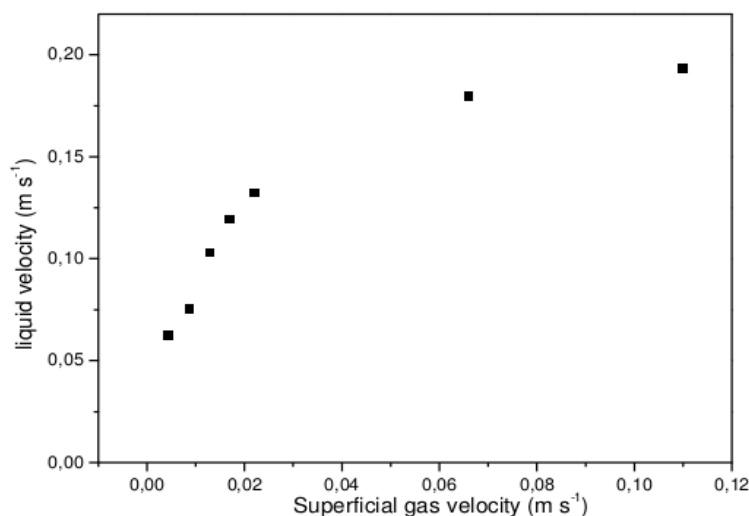
Figure 5. Simulations results data for liquid velocity

5. CONCLUSIONS

In the present study, the effects of reactor geometry on the hydrodynamic parameters in an internal airlift reactor were investigates theoretically using CFD. Special attention was given to the liquid circulation velocity and the gas holdup in the riser. An important parameter in airlift reactors is the location and type of sparger used to introduce gas into the reactor. With the results obtained, it can be concluded that the location of the sparger, in the gap between the cylinders, possible to obtain adequate values of gas holdup close to those found in the literature. Experiments are being conducted in order to compare the results of these simulations with those obtained in the reactor benchtop.

6. ACKNOWLEDGEMENTS

7. REFERENCES

Chisti, Y., 1998. "Pneumatically agitated bioreactors in industrial and environmental bioprocessing: hydrodynamics, hydraulics, and transport phenomena". *Applied Mechanics Reviews*, Vol. 51, (1), p. 33–112.

Ebrahimifakhari, M, Mohsenzadeh, E., Moradi, S, Moraveji, M. and Salami, M., 2011. "CFD simulation of the hydrodynamics in an internal air-lift reactor with two different configurations". *Frontiers of Chemical Science and Engineering*. Vol. 5, (4), p. 455–462.

van Baten, J.M. and Krishna, R, 2003. "Comparison of Hydrodynamics and Mass Transfer in Airlift and Bubble Column Reactors Using CFD". *Chemical Engineering and Technology*. Vol. 26, (10), p. 1074-1079.

Simcık, M., Mota, A., Ruzicka, M.C, Vicente, A. and Teixeira, J. "CFD simulation and experimental measurement of gas holdup and liquid interstitial velocity in internal loop airlift reactor". *Chemical Engineering Science*, Vol. 66, p. 3268–3279.

Wasewar, K.L; Anil, M. and Agarwal, V.K., 2008. "CFD Modeling of Three-phase Bubble Column: 2. Effect of Design Parameters". *Chemical and Biochemical Engineering Quarterly*, Vol. 22, (2), p. 143–150.

Zhang, T., Wei, C., Feng, C. and Zhu, J., 2012. "A novel airlift reactor enhanced by funnel internals and hydrodynamics prediction by the CFD method". *Bioresource Technology*, Vol. 104, p. 600–607.

dos Santos, C. M., 2005. "Simulação Tridimensional com Sistema Gás-Líquido em Colunas de Bolhas". (In Portuguese). Dissertação UNICAMP, 2005. 120 pp.

van Benthum, W.A.J., Van der Lans, R.G.J.M. and Van Loosdrecht; Heijnen, J. J., 1999. "Bubble recirculation regimes in an internal-loop airlift reactor". *Chemical Engineering Science*, Vol. 54, p. 3995-4006.

Chisti, Y. and Jauregui-Haza, U.J., 2002. "Oxygen transfer and mixing in mechanically-agitated airlift bioreactors". *Biochemical Engineering Journal*, Vol. 10, p. 143-153.